PRAMANA
— journal of
physics

Vol. xx, No. x
xxxx xxxx
pp. 1–12

Recent RHIC results on photon, dilepton and heavy quarks

Frédéric Fleuret
Laboratoire Leprince-Ringuet, École polytechnique, CNRS/IN2P3, 91128 Palaiseau, France

Abstract. We present here a review of the recent results obtained by the RHIC experiments in the framework of QCD under extreme conditions of high temperature or large baryon density, the so called Quark Gluon Plasma. We focus on a specific categories of observable: the electromagnetic probes which cover a large spectrum of experimental studies.

Keywords. QGP, RHIC, photon, vector meson, thermal dilepton, heavy quarks

PACS Nos 2.0

1. Introduction

The understanding of QCD under extreme conditions of high temperature or large baryon density has been a subject of extreme interest along the past thirty years. This high energy density state called Quark Gluon Plasma (QGP) should be characterized by a strongly reduced interaction between its constituents, the partons. Lattice QCD predicts a phase transition from the normal nuclear matter to a QGP at a temperature of approximately T $\approx$ 170 MeV $\approx 10^{12}$ K, corresponding to an energy density $\varepsilon \approx$1 GeV/fm^3, nearly an order of magnitude larger than that of normal nuclear matter.

Experimentally, the search of the QGP has been performed by studying ultrarelativistic heavy ion collisions, first at Bevalac-LBNL (1975 - 1985) at $\sqrt{s_{NN}} \approx$ 1 GeV, then at AGS-BNL (1987 - 1995) at $\sqrt{s_{NN}} \approx$ 5 GeV and at SPS-CERN (1987 - present) at $\sqrt{s_{NN}} \approx$ 17 GeV. Since 2000, the Relativistic Heavy Ion Collider (RHIC) at BNL performs proton and ion collisions at an energy up to $\sqrt{s_{NN}} \approx$ 200 GeV. Table 1 shows a summary of the first 8 years of PHENIX data taking, one of the two larger experiments (PHENIX and STAR) among the four experiments (PHENIX, STAR, BRAHMS and PHOBOS) running at RHIC.

Among the observables used to study heavy ion collisions, electromagnetic probes play a special role since they have the definite advantage of suffering little or no final state interaction. They thus open a window to the hot and dense phase of the reaction.

Electromagnetic radiations can be sorted in several categories: direct photons which give information on thermal radiation, low mass vector mesons which give information on the modification of hadron properties in a dense medium and its relation to chiral symmetry restoration, thermal dileptons, heavy quark continuum and heavy quark resonances.

Table 1. Integrated luminosity recorded by the PHENIX experiment since 2000.

year	run	species	integrated luminosity
2000	1	Au+Au (130 GeV)	1 μb^{-1}
01/02	2	Au+Au (200 GeV) / p+p (200 GeV)	24.0 μb^{-1} / 0.15 pb^{-1}
02/03	3	d+Au (200 GeV) / p+p (200 GeV)	2.74 nb^{-1} / 0.35 pb^{-1}
03/04	4	Au+Au (200 GeV) / Au+Au (62 GeV)	241 μb^{-1} / 9 μb^{-1}
04/05	5	Cu+Cu (200 GeV) / Cu+Cu (62 GeV)	3 nb^{-1} / 0.19 nb^{-1}
		Cu+Cu (22.5 GeV) / p+p (200 GeV)	2.7 μb^{-1} / 3.8 pb^{-1}
05/06	6	p+p (200 GeV)	10.7 pb^{-1}
06/07	7	Au+Au (200 GeV)	813 μb^{-1}
07/08	8	d+Au (200 GeV) / +p (200 GeV)	80 nb^{-1} / 5.2 pb^{-1}

Figure 1 gives a schematic view of this sorting. It shows the invariant mass distribution of a dilepton spectrum. Photons stand at 0. Low mass region, between 0 and 1 GeV/c, gives access to vector mesons in medium. Intermediate mass region, between 1 and 2.5 GeV/c, corresponds to thermal dileptons and heavy quarks continuum. Finally, above 2.5 GeV/c, one access to heavy quarks resonances. This paper will be articulated following this classification ; we will then successively review:

- Photons
- Vector mesons in medium and thermal dileptons
- Heavy quarks continuum
- Heavy quarks resonances

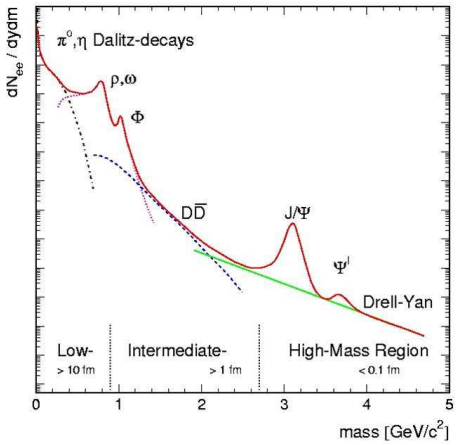

Figure 1. Dielectron invariant mass distribution and its classification in different mass regions.

In the following, we will often consider results from $p+p$ and $p(d)+A$ together with $A+A$. The interest in studying $p+p$ and $p(d)+A$ collisions is driven by the necessity to compare $A+A$ collisions with a baseline reference in order to identify initial state effects and final state effects. We will often refer to the nuclear modification factor R_{AB} which

compares the results obtained in $A + A$ to a simple superposition of $A \times A$ nucleon-nucleon collisions:

$$R_{AA} = \frac{dN^X_{AA}}{\langle N_{coll} \rangle \times dN^X_{pp}} \tag{1}$$

where dN^X_{AA} and dN^X_{pp} are respectively the yield of particle X observed in A+A collisions and p+p collisions, and $\langle N_{coll} \rangle$ is the average number of nucleon-nucleon collisions occuring in a A+A collision. In absence of nuclear effect the R_{AA} ratio should equal unity.

2. Photons

Photons emitted in the course of a heavy-ion reaction has long been considered a priviledge probe of the space-time evolution of the colliding system. Study of direct photons is especially interesting since they are emmitted from all the states of the heavy ion collisions and, due to their weak interaction with the medium, are not distorded by final-state interctions . The term direct photons is used to indicate photons that emerge directly from a particle collision, in contrast with decay photons which emerge as the daughters of long-lived particles such as $\pi^0 \rightarrow \gamma\gamma$.

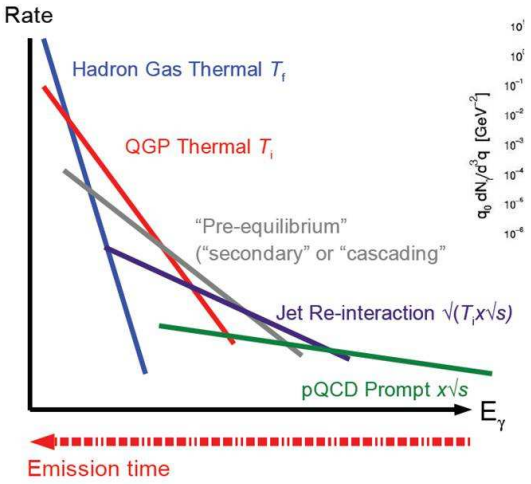

Figure 2. Direct and fragmentation photon relative contribution

Direct photons produced in a heavy ion reaction are emitted at various stages with several contribution processes as shown in Figure 2. At high p_T (large E_γ), photons are produced in initial parton-parton scatterings with large momentum transfer. At low p_T, a significant fraction of photons is expected to come from the thermalized medium. These so-called thermal photons can come either from the hadron gas or the QGP. At intermediate p_T, the interaction of quarks and gluons from hard processes with the dense medium can be a significant source of direct photons.

Photons produced in initial parton-parton scatterings have been studied in p+p and d+Au collisions. Figure 3 shows the results obtained by the PHENIX experiment in both run 3 [1]

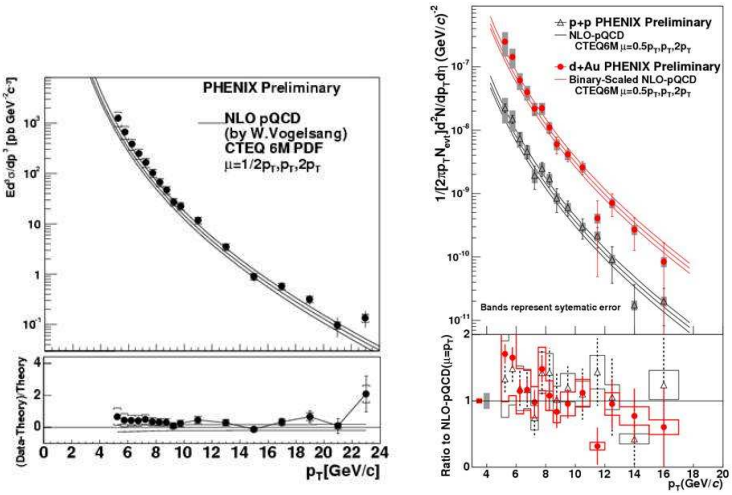

Figure 3. Direct photon spectra measured by the PHENIX exepriment compared with NLO pQCD calculations. Left: p+p run 5 data; right: p+p and d+Au run 3 data.

and run 5 (preliminary results). They show a fair agreement between data and NLO pQCD calculations for both p+p and d+Au samples. Beside the fact that these results demonstrate the robustness of the pQCD description of direct photon production, they show that, within experimental uncertainties, no nuclear effects seem to affect direct photon production in d+Au collisions.

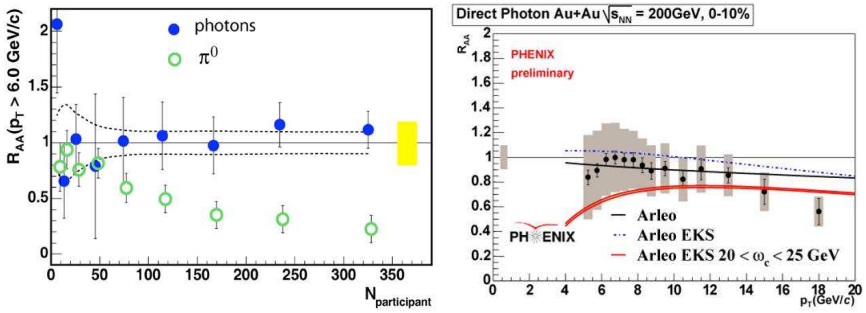

Figure 4. Left: Ratio of Au+Au yield to p+p yield normalized by the number of binary collisions as a function of centrality given by $N_{\rm part}$.

Figure 4 shows the nuclear modification factor R_{AA} of direct photon as measured by PHENIX in Au+Au collisions in run 2 [2] and run 4 (preliminary). The left plot shows the centrality dependence of the high p_T production as a function of the number of participating nucleons. High p_T direct photon production in Au+Au collisions is well described by the p+p direct photon yield scaled by the average number of collisions, indicating that,

whithin experimental uncertainties, no nuclear effect seems to affect the direct photon production. Thus, the direct photon production in $A + A$ collisions can be described as a simple superposition of $A \times A$ single nucleon+nucleon interactions. However, a closer look at the most central $Au + Au$ collisions shows some deviation to R_{AA}= 1: Right plot of figure 4 shows the R_{AA} as a function of p_T for the run 4 $Au + Au$ data. This plot corresponds to the 10% most central collisions. One can see a deviation from R_{AA}=1 at large p_T. This behaviour can be described in the context of nuclear shadowing [3].

2.2 Thermal photons

As seen in previous section, high p_T photon spectra are well described by pQCD NLO calculations in both $p + p$ and $A + A$ collisions. Extending NLO pQCD calculations to lower p_T offer the opportunity to study thermal photon production in central $Au + Au$ collisions; Figure 5 shows the 10 % more central collisions compared to a hydrodynamical model that includes NLO pQCD calculations, hadron resonance gas thermal photon emission and QGP thermal photon emission. A clear excess of thermal photons is ob-

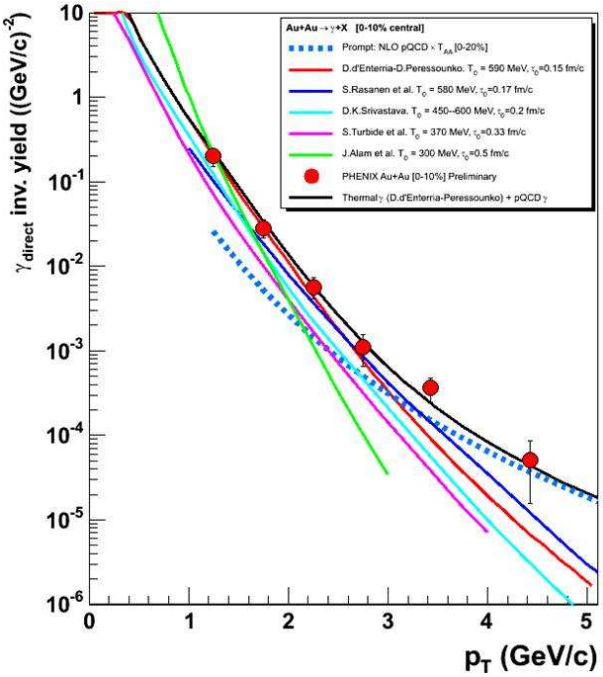

Figure 5. Direct photon invariant yield measured by PHENIX in the 10 % most central Au+Au collisions. Dashed curve corresponds to pQCD calculations. Colored curves correspond to hydrodynamical models.

served at low p_T. Fitted to the data, this excess leads to a maximum temperature reached in a nucleus-nucleus reaction close to 250 MeV as stated in [4], well above the expected temperature needed to produce a Quark-Gluon Plasma.

3. Vector mesons in medium and thermal dileptons

Emission from a hot and dense matter are expected to include thermal radiations as well as in-medium decays of mesons with short lifetime. The discovery of a large enhancement of the dilepton yield at masses below the Φ meson mass in ion-ion collisions at CERN SPS [5] has triggered theoretical efforts on the modification of the hadron properties in a dense medium and its relation to chiral symmetry restoration [6]. Above the Φ meson mass, an ehancement yield was also observed. Preliminary NA60 data suggest that this enhancement may results from prompt production, as expected from thermal radiation [7].

The PHENIX experiment has extended these measurements by studying dielectron pro-

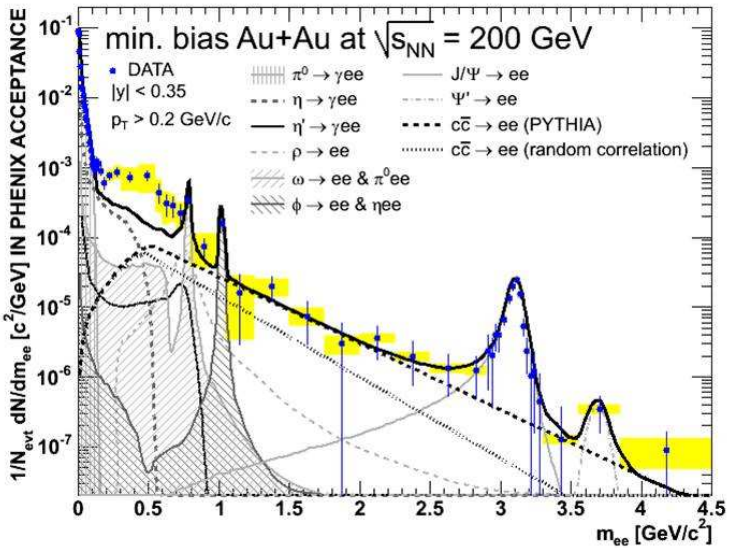

Figure 6. Invariant e^+e^- pair yield measured by PHENIX in Au+Au collisions compared to the yield from the model of hadron decays.

duction in Au+Au collisions at $\sqrt{s_{NN}}$= 200 GeV [8] . Figure 6 shows the dielectron invariant yield as a function of the dielectron invariant mass after subtraction of a large uncorrelated combinatorial background. The data below 150 MeV/c^2 are well described by a cocktail of hadronic sources. However, a large excess is observed in the continuum region between 150 and 750 MeV/c^2, a factor more than 3 when compared to the expected yield. Above the Φ meson mass, the data are well described by the correlated open charm continuum calculation. Assuming that this correlation is canceled out by hot and dense matter effect leads to a much smaller contribution (stated as $c\bar{c} \to ee$ random correlation on the plot) thus leaving significant room for e.g. thermal radiations.

Figure 7 shows the centrality dependence of the yield for three mass regions: Below 100 MeV/c^2, from 150 to 750 MeV/c^2 and 1.2 to 2.8 GeV/^{2}. The yield of the first two regions is normalized to the number of participating nucleon pairs ($N_{\rm part}$/2). The last one is normalized by the number of binary collisions as expected for hard processes. The expectations from hadron cocktail are also plotted. At low mass, below 100 MeV/c^2, data agree with expectation as seen on Figure 6. In the second mass region, from 150 to 750

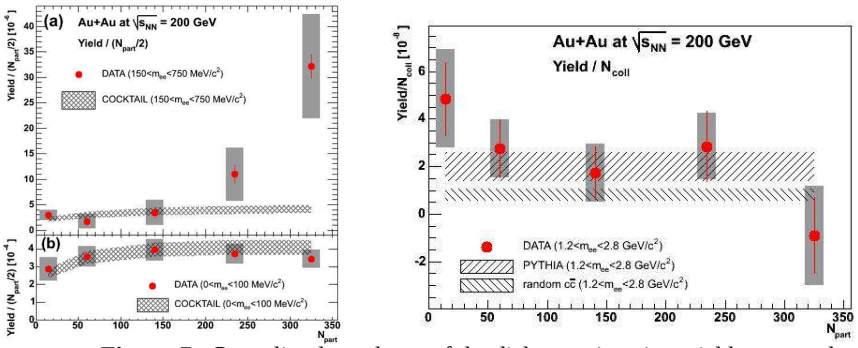

Figure 7. Centrality dependence of the dielectron invariant yield compared to expectations for three mass regions.

MeV/c^2, the excess rises with the centrality of the collision, supporting the conjecture of an enhancement due to in-medium effects. In the range from 1.2 to 2.8 GeV/^{2}, no significant centrality dependence is observed and the data are consistent with correlated open charm expectation as already seen in Figure 6. As in Figure 6 a global excess is observed when compared to uncorrelated open charm expectations.

4. Open charm

Heavy quarks (charm or bottom) open a priviledge window to the properties of the hot and dense medium created in $A + A$ collisions. Due to their large mass a larger thermalization time is expected thus leading to a smaller suppression of their high p_T yield and a smaller elliptic flow than for π^0 and other hadrons. Both STAR [9] and PHENIX [10] experiments

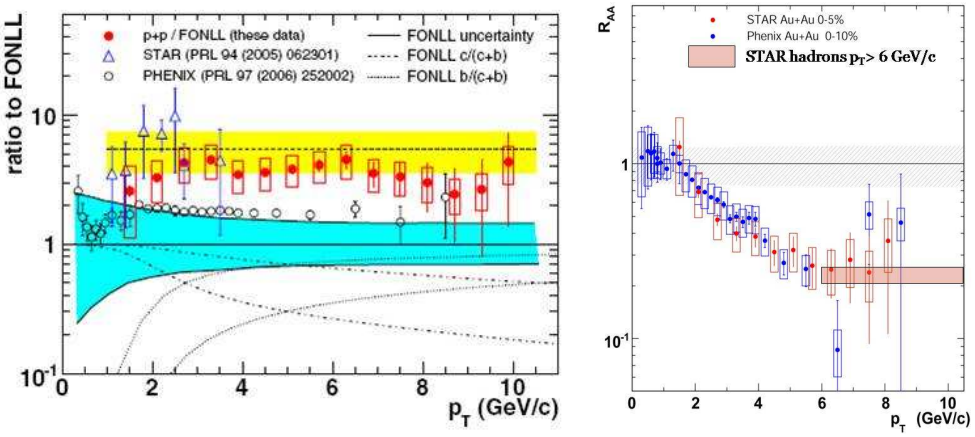

Figure 8. Open charm production in p+p (left plot) and most central Au+Au (right plot) collisions as measured by PHENIX and STAR.

have studied open charm production via nonphotonic electron yield. Figure 8 shows the nonphotonic electron yield measured by both experiments in $p+p$ and $Au+Au$ collisions. The $p+p$ measurements is presented as the ratio of measured to unscaled FONLL nonphotonic electron yield. The FONLL calculation underestimate both measurements (by a factor 2 for PHENIX data, by a factor 4 for STAR data). In addition, the results of both experiments are not consistent with each other. Note though that the shape of the p_T spectra seems in agreement with theoretical expectations.

The $Au+Au$ data shown in Figure 8 are presented as the R_{AA} ratio as a funtion of p_T for most central collisions. In contrast with $p+p$ data, both experiments agree well within experimental uncertainties, meaning that the discrepancy observed in $p+p$ does also exist with the same amplitude in $Au+Au$ and cancels out in the ratio. The suppression observed in the $Au+Au$ R_{AA} reaches the same suppression as light hadrons for central $Au+Au$ collisions at a p_T around 6 GeV/c, indicating that high p_T heavy quarks are strongling coupled to the medium.

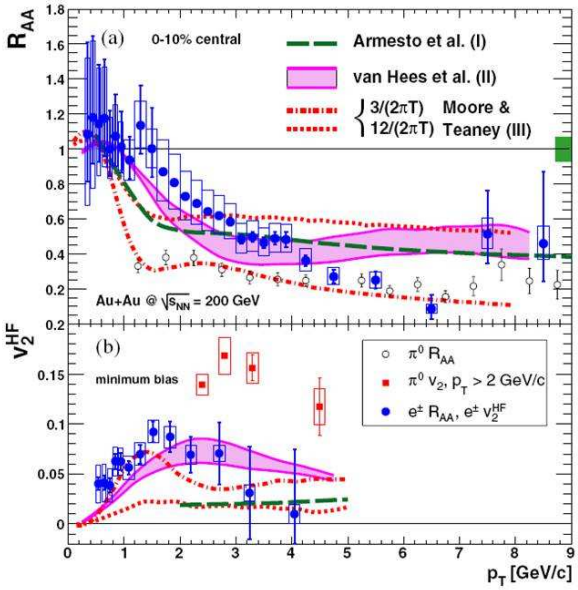

Figure 9. Heavy quark R_{AA} (top plot) and v_2 (bottom plot) as a function of p_T measured by PHENIX in the 10 % most central Au+Au collisions.

The PHENIX experiment as also measured $v_2(p_T)$, the azimuthal anisotropy, which is, as energy loss, related to the transport properties of the medium. Figure 9 shows that a large v_2^{HF} is observed, indicating that the charm relaxation time is comparable to the short time scale of flow development in the produced medium. This is another indication that heavy quarks are strongly coupled to the medium and reinforce the conclusion that hot and dense medium is produced in central $Au+Au$ collisions.

5. Heavy Quarks resonances

As first predicted by Matsui and Satz [11], the suppression of charmonia production is expected to be an unambigous signature for the formation of a QGP. A first anomalous J/ψ suppression, increasing with the centrality of the collision, has been observed by the NA50 experiment at CERN/SPS in Pb+Pb collisions at $\sqrt{s_{NN}} = 17.3$ GeV, leading to an intense theoretical work. At RHIC, the PHENIX experiment has measured the J/ψ production in p+p, d+Au, Cu+Cu and Au+Au collisions at $\sqrt{s_{NN}} = 200$ GeV. The PHENIX experiment measures J/ψ via its dielectron decay within the mid-rapidity region $|y| < 0.35$ and its dimuon decay at forward and backward rapidity $1.2 < |y| < 2.2$. In order to study "anomalous" suppression induced by Hot and Dense Matter effects, the Cold Nuclear Matter (CNM) effects must be understood. These last effects are studied with p+p and d+Au results.

5.1 Cold Nuclear Matter effects

The p+p measurement defines the baseline to study nuclear effects. It is used to compute the nuclear modification factor R_{AB}:

$$R_{AB} = \frac{dN_{AB}^{J\psi}}{\langle N_{coll} \rangle \times dN_{pp}^{J/\psi}} \tag{2}$$

where $dN_{AB}^{J/\psi}$ and $dN_{pp}^{J/\psi}$ are respectively the J/ψ yield observed in A+B collisions and p+p collisions, and $\langle N_{coll} \rangle$ is the average number of nucleon-nucleon collisions occuring in a A+B collision. Figure 10 shows the J/ψ transverse momentum and rapidity spectra obtained by PHENIX in p+p collisions [12].

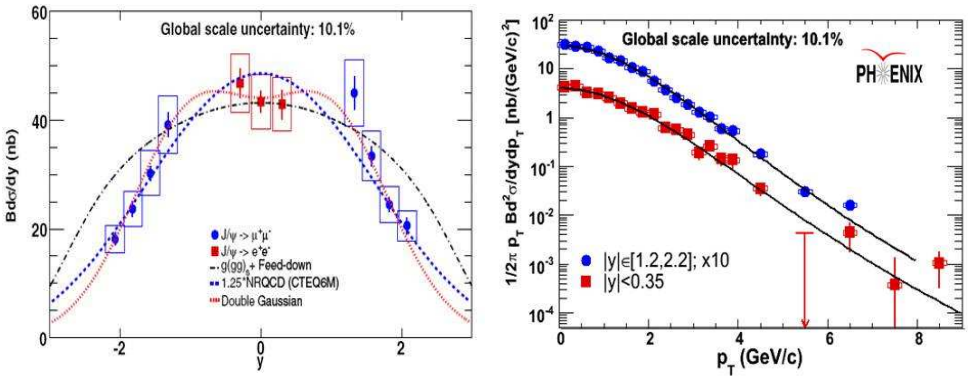

Figure 10. J/ψ rapidity (left plot) and transverse momentum (right plot) spectra measured by the PHENIX experiment in p+p collisions.

As previously mentionned, the d+Au data (where HDM effects are not supposed to occur) give information about CNM effects. Two process are usually considered as contributing to the CNM effects : gluon shadowing which induces a modification of the parton structure functions and nuclear absorption (or nuclear breakup) which comes from the fact

that J/ψ's are produced in nuclei and can thus interact with the surrounding nucleons [1]. Figure 11 shows R_{dAu} (the R_{AB} ratio for d+Au collisions) as a function of the rapidity [15]. It exhibits modest CNM effects which can fairly be reproduced by models incorporating weak gluon shadowing and weak nuclear absorption.

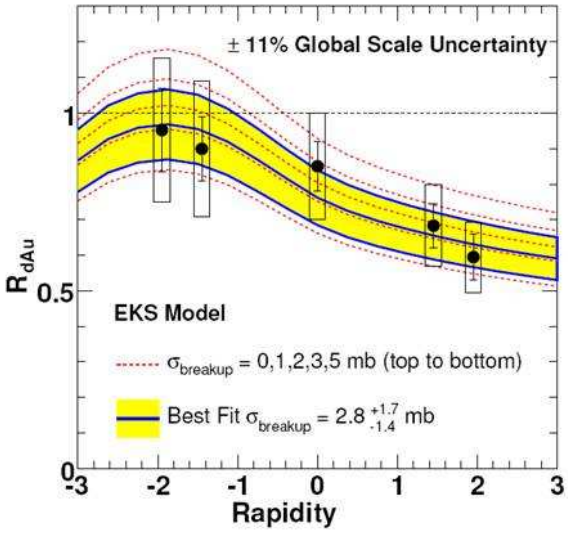

Figure 11. J/ψ $R_{d\mathrm{Au}}$ as a function of rapidity compared to EKS shadowing modelisation with several values of nuclear breakup cross section.

5.2 Comparison between RHIC and SPS

Figure 12 shows a comparison of the results obtained at $\sqrt{s_{NN}} = 200$ GeV at RHIC with the results obtained at lower energies ($\sqrt{s_{NN}} \sim 20$ GeV) at CERN by the NA50 [13] and NA60 [14] experiments. On the experimental point of view, without taking into account any CNM effect, the results obtained at both energies are similar. At CERN, the CNM effects are well reproduced with a 4.18 mb absorption cross section (without including any gluon shadowing effect). At RHIC, the suppression pattern due to CNM effects could be similar, but due to the poor precision of the d+Au experimental data, the CNM effects at RHIC are not well constrained, and it is so far difficult to draw a clear conclusion. The recent d+Au data taken in 2008 at RHIC with 30 times more statistic than currently available should help to disentangle between the different scenarios of CNM effects at RHIC.

[1] This last effect is well established. At SPS energies, the absorption cross section has been measured to be 4.18 ± 0.35 mb [13].

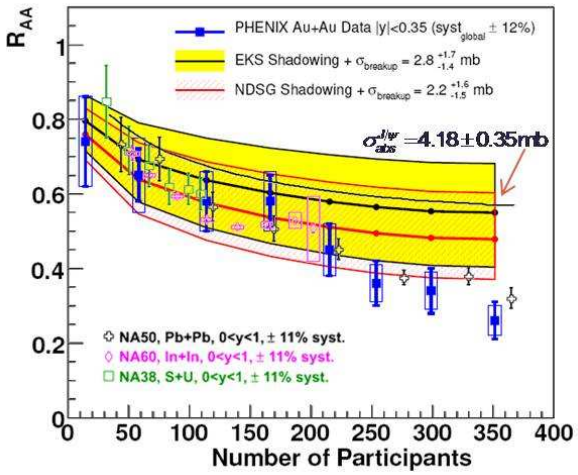

Figure 12. J/ψ R_{AA} as a function of centrality for PHENIX mid-rapidity Au+Au collisions compared to CERN NA38, NA50 and NA60 results at $\sqrt{s_{NN}} \sim 20$ GeV.

5.3 Comparison with models

Several models have been proposed to accomodate the results obtained both at SPS and RHIC. In a first attempt, the models which have been used to fit SPS data have been extended to RHIC data. The left plot of figure 13 shows Au+Au PHENIX results [16] and their comparison with several theoretical curves corresponding to different suppression process (citations). In all cases, the expected suppression is overestimated when comparing to the data, suggesting that new mechanisms could be at work, such as J/ψ regeneration.

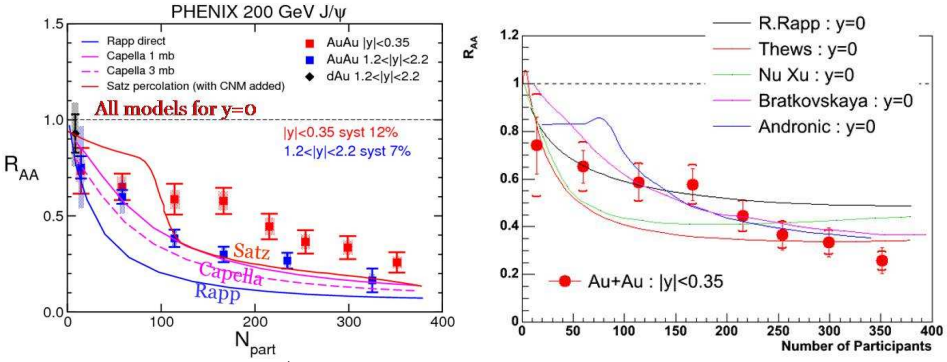

Figure 13. J/ψ PHENIX data compared to models which fit SPS data (left plot) and recombination models (right plot).

Regeneration models which are based on the idea that in a medium such as QGP, if several c and $\bar{c}$ quarks are produced, then a c quark from one initial $c\bar{c}$ pair can interact with

a $\bar{c}$ quark from a different initial $c\bar{c}$ pair to from a J/ψ, thus leading to an increase of the net J/ψ production cross section. The number of J/ψ formed via such interactions is expected to be proportional to the number of $c\bar{c}$ combinations, which is roughly proportional to the square of the number of the $c\bar{c}$ pairs [17]. At CERN energies, this process doesn't occur since around 0.1 $c\bar{c}$ are produced, on average, in each collision. At RHIC energies, the amount of $c\bar{c}$ pairs produced in a collision is larger than 10. Right plot of Figure 12 shows central rapidity PHENIX Au+Au results and their comparison with several models which include regeneration process. Even though the data are not fully well described, the agreement is much better than without any regeneration mechanism interplay at RHIC energies.

6. Conclusion

In conclusion, the RHIC experiments have provided important results in the long range study of the Quark Gluon Plasma. Electromagnetic probes which are considered as priviledge probes for the study of such a state of matter plead in favor of the production of a strongly coupled hot and dense medium in central $Au + Au$ collisions, but several questions remain unanswered. At RHIC, Future data taking together with detector upgrades will give new crucial information. In a near future, the beginning of LHC era will open a new region of investigation, giving us the hability to extend the studies already made at AGS, SPS and RHIC.

References

[1] S.S. Adler *et al.* (PHENIX Collaboration), Phys. Rev. Lett. **98**, 012002 (2007).
[2] S.S. Adler *et al.* (PHENIX Collaboration), Phys. Rev. Lett. **94**, 232301 (2005).
[3] F. Arleo, JHEP 0609, 015 (2006).
[4] D. d'Enterria and D. Peressounko, Eur. Phys. J. C**46**, 451 (2006).
D. d'Enterria, J. Phys. G**34**: S53-S82 (2007).
[5] G. Agakishiev *et al.*, Phys. Rev. Lett. **75**, 1272 (1995).
[6] R. Rapp, J. Wambach, Adv. Nucl. Phys. **25**, 1 (2000).
[7] R. Shahoian *et al.*, PoS **HEP2005**, 131 (2006).
[8] S. Afanasiev *et al.* (PHENIX Collaboration), arXiv:0706.3034 (2007).
[9] B. I. Abelev *et al.* (STAR Collaboration), Phys. Rev. Lett. **98**, 192301 (2007).
[10] A. Adare *et al.* (PHENIX Collaboration), Phys. Rev. Lett. **98**, 172301 (2007).
[11] Matsui and Satz, Phys. Lett. **B178**, 416 (1986).
[12] A. Adare *et al.* (PHENIX Collaboration), Phys. Rev. Lett. **98**, 232002 (2007).
[13] B. Alessandro *et al.* (NA50 collaboration), Eur. Phys. Jour. **C39**, 335 (2005).
[14] R. Arnaldi *et al.* (NA60 collaboration), Nucl. Phys. **A774**, 719 (2006).
[15] A. Adare *et al.* (PHENIX Collaboration), Phys. Rev. C **77**, 024912 (2008).
[16] A. Adare *et al.* (PHENIX Collaboration), Phys. Rev. Lett. **98**, 232301 (2007).
[17] GrandChamp *et al.*, Phys. Rev. Lett. **92**, 212301 (2004). Thews and Mangano, Phys. Rev. **C73**, 014904 (2006).